Atmospheric Environment 186 (2018) 189–197

Contents lists available at ScienceDirect

Atmospheric Environment

journal homepage: www.elsevier.com/locate/atmosenv

Modeling dispersion of emissions from depressed roadways

Seyedmorteza Amini[a], Faraz Enayati Ahangar[a], David K. Heist[b], Steven G. Perry[b], Akula Venkatram[a,*]

[a] Department of Mechanical Engineering, University of California, Riverside, CA 92521, USA
[b] Atmospheric Modeling and Analysis Division, National Exposure Research Laboratory, MD-81, U.S. Environmental Protection Agency, Research Triangle Park, NC 27711, USA

ARTICLE INFO

Keywords:
Near-road air quality
Dispersion modeling
Depressed roadway
Wind tunnel experiment
Roadway configurations

ABSTRACT

This paper presents an analysis of data from a wind tunnel (Heist et al., 2009) conducted to study dispersion of emissions from three depressed roadway configurations; a 6 m deep depressed roadway with vertical sidewalls, a 6 m deep depressed roadway with 30° sloping sidewalls, and a 9 m deep depressed roadway with vertical sidewalls. The width of the road at the bottom of the depression is 36 m for all cases. All these configurations induce complex flow fields, increase turbulence levels, and decrease surface concentrations downwind of the depressed road compared to those of the at-grade configuration. The parameters of flat terrain dispersion models are modified to describe concentrations measured downwind of the depressed roadways. In the first part of the paper, a flat terrain model proposed by van Ulden (1978) is adapted. It turns out that this model with increased initial vertical dispersion and friction velocity is able to explain the observed concentration field. The results also suggest that the vertical concentration profiles of all cases under neutral conditions are best explained by a vertical distribution function with an exponent of 1.3. In the second part of the paper, these modifications are incorporated into a model based on the RLINE (Snyder et al., 2013) line-source dispersion model. While this model can be adapted to yield acceptable estimates of near-surface concentrations ($z < 6$ m) measured in the wind tunnel, the Gaussian vertical distribution in RLINE, with an exponent of 2, cannot describe the concentration at higher elevations. Our findings suggest a simple method to account for depressed highways in models such as RLINE and AERMOD through two parameters that modify vertical plume spread.

1. Introduction

Living and working near major roadways has been associated with increased risk of respiratory complications, cardiovascular disease, and other adverse health effects (Health Effects Institute, 2010). Several configurations have been suggested to mitigate the near-road impact of vehicle emissions. These configurations include depressed and elevated roadways, and roadways with sound walls and/or vegetation barriers.

A relatively small number of studies have examined dispersion of emissions from depressed roadways. A notable field study was conducted in the Los Angeles Air Basin by the California Department of Transportation (CalTrans) to collect data to understand dispersion of primary pollutants emitted from freeways with various configurations, including at-grade, depressed, and elevated roads (Bemis et al., 1977). Air pollutants sampled included CO, reactive and unreactive hydrocarbons, NOx, O_3, SO_2, and H_2S. Particulate sampling was also conducted to obtain total particulates and lead.

The data from the CalTrans field study (Bemis et al., 1977) were used to develop the depressed road model in the California Line Source Dispersion Model (CALINE2). CALINE, which is used to estimate air pollutant concentrations near roadways, accounts for the effects of road depression by enhancing the initial vertical plume spread relative to those used for equivalent at-grade sites (Bemis et al., 1977; Benson, 1992).

Feeney et al. (1975) measured aerosols and particulate lead concentrations in the vicinity of several road configurations, including a depressed roadway. Samplers were placed 20 m upwind of a freeway and at several distances downwind of the freeway ranging from 27 m to approximately 160 m from the median strip. They found that the mass concentrations of traffic-derived lead were generally lower downwind of the depressed roadway relative to that predicted by a dispersion model that assumed that the emissions occurred at road level.

Heist et al. (2009) conducted a comprehensive wind-tunnel study on dispersion of emissions from model depressed roadways. The studied configurations included a flat roadway, a 6 m and a 9 m deep depressed roadway with vertical sidewalls, a 6 m deep depressed roadway with

* Corresponding author.
E-mail address: venkatram@sbcglobal.net (A. Venkatram).

https://doi.org/10.1016/j.atmosenv.2018.04.058
Received 12 July 2017; Received in revised form 18 April 2018; Accepted 29 April 2018
Available online 01 May 2018

30° sloping sidewalls, and a 6 m deep depressed roadway with 30° sloping sidewalls with two 6 m solid barriers on top of the road. They observed that all these configurations alter the flow field, increase downwind dispersion, and reduce downwind surface concentrations relative to the flat terrain case. The level of reduction in concentrations depended on the particular configuration.

Baldauf et al. (2013) conducted a field study in Las Vegas, Nevada, to investigate the effects of a depressed roadway on local-scale air quality downwind of the depression. They measured CO and NO_x concentrations along a complex urban highway at two sections; a section at-grade with the surroundings and another section that was depressed. The vertical height from the roadbed to the top of the surroundings was 5 m, and the slope of the sidewalls was approximately 20°. The stationary monitors located 20 m from the downwind edge of the freeway at both sections showed that the maximum concentrations occurred at the at-grade site. However, during some mid- and low-concentration events, the stationary monitor downwind of the cut section observed higher concentration levels than that of the at-grade section. The mobile monitoring data collected along the at-grade and cut section transects indicated that the concentrations at the at-grade transect were greater than those at the cut section transect at 35 m from the downwind edge of the freeway, with concentrations then becoming similar along both gradients further downwind of the highway. They also conducted a wind tunnel simulation of the study site to examine the flow field and the concentration distributions in the vicinity of the highway. The wind tunnel simulations revealed that the cut section reduced concentrations of pollutants measured at breathing-level height by 15–25% relative to the flat terrain case for receptors located approximately 20 m from the downwind edge of the highway. Although the field data were not conclusive, the data collected under the controlled conditions of the wind tunnel indicated that depressed roadways led to reductions in downwind near-surface concentrations relative to those next to at-grade roadways.

Until recently, CALINE3 (and more refined models such as CAL3QHC and CAL3QHCR) had been recommended by the United States Environmental Protection Agency (U.S. EPA) to be used to estimate the impact of vehicular emissions on near-road air concentrations. The situation changed in 2016 when the U.S. EPA replaced CALINE3 with American Meteorological Society/U.S. EPA Regulatory Model (AERMOD) for Transportation Related Air Quality Analyses (U.S. Environmental Protection Agency, 2016). However, AERMOD designed primarily for point, area, and volume-type pollutant sources does not simulate the line-type sources explicitly; line sources are represented as elongated area sources or a series of volume sources evenly spaced along the length of the lines (Heist et al., 2013). AERMOD is also not currently configured to model concentrations downwind of roadways with complex geometries.

In an effort to develop a comprehensive line source dispersion model, the U.S. EPA formulated the Research LINE source model (RLINE) (Snyder et al., 2013). The model framework is designed to facilitate the inclusion of algorithms for complex road geometries, therefore providing a suitable testbed for potential depressed roadway approaches. This study provides results that can be used to incorporate depressed roadways in RLINE.

In this study, we analyze the concentrations and turbulence levels measured in the wind tunnel study downwind of at-grade and depressed road configurations (Heist et al., 2009) to gain insight into the processes that govern dispersion of pollutants from a depressed highway. Wind tunnel studies can provide more information on the processes than field studies can because the governing inputs are controlled and details of the flow fields can be measured. Although they do have the disadvantage of being unable to simulate the effects of atmospheric stability, they provide information that is vital to the development of models for situations in which the effects of source geometry on the flow field are dominant. For example, the wind tunnel results (Heist et al., 2009) on dispersion of pollutants downwind of the roadways with different configurations have been incorporated into several dispersion and CFD models (Ahangar et al., 2017; Amini et al., 2017, 2016; Ghasemian et al., 2017; Hagler et al., 2011; Schulte et al., 2014; Steffens et al., 2014).

Based on the insight from the wind tunnel study, we propose a method to incorporate the dominant effects of the depressed roadway into a flat terrain model. These effects are first parameterized in a model proposed by van Ulden (1978) which not only provides a good description of ground-level concentrations but also the vertical profiles (Nieuwstadt and van Ulden, 1978a; b) measured during the Prairie Grass experiment (Barad, 1958). We then suggest how our findings can be incorporated into a model based on the formulation of RLINE, a Gaussian dispersion model, with emphasis on near-surface concentrations.

2. Wind tunnel experiments

2.1. Experiment description

Heist et al. (2009) performed an experimental study in the U.S. EPA's Meteorological Wind Tunnel (Snyder, 1979) to explore the effects of different road configurations on the dispersion of traffic-related pollutants downwind of roads. The wind tunnel test section is 3.7 m wide, 2.1 m high, and 18.3 m long. A simulated atmospheric boundary layer was generated using three truncated triangular (Irwin, 1981) spires mounted near the entrance to the test section. To maintain the boundary layer, the floor of the test section downwind of the spires was covered with roughness blocks. The position of spires and roughness blocks are shown in Fig. 1. There are no roughness blocks in the proximity of the line sources where turbulence and concentration measurements are conducted. The modeled freeway is a six lane divided highway at 1:150 scale. The width of the modeled freeway is 36 m full scale. The origin of the coordinate system is at the center of the roadway on the wind tunnel floor, with the positive x in the stream wise direction, y along the axis of the roadway, and z vertically upward. The wind-tunnel study examined twelve roadway configurations. In this paper, we focus on three depressed roadway configurations and compare the results to those of a flat roadway.

The configurations that were studied in this paper are shown in Fig. 2. We examine a 6 m deep depressed roadway with vertical sidewalls (D690), a 6 m deep depressed roadway with 30° angled sidewalls

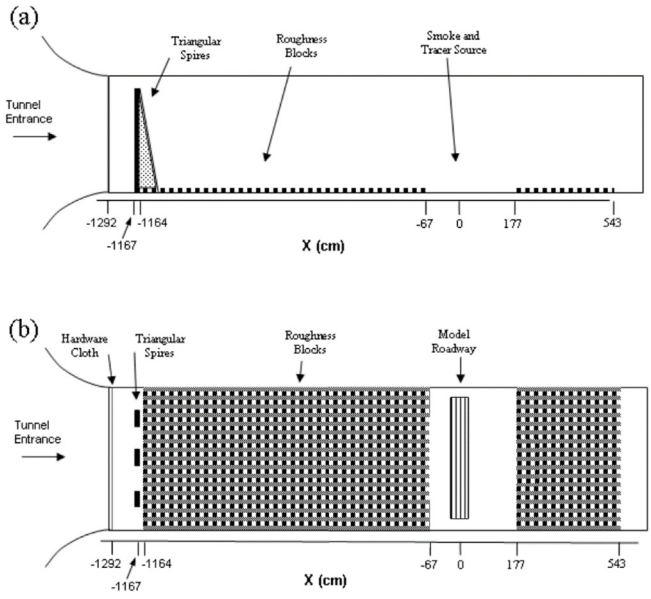

Fig. 1. Schematic of near roadway wind tunnel setup: a) elevation and b) plan view.

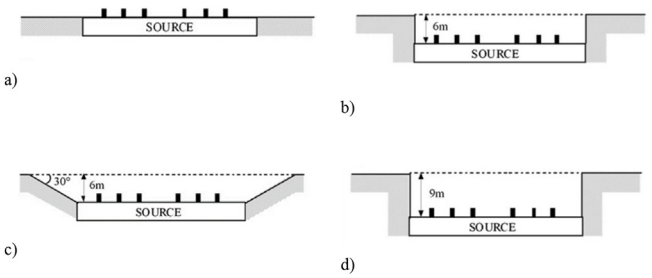

Fig. 2. Elevation view showing cross sections through the different roadway designs studied; a) flat terrain roadway (FLAT), b) 6 m deep depressed roadway with vertical sidewalls (D690), c) 6 m deep depressed roadway with 30° sloping sidewalls (D630), and d) 9 m deep depressed roadway with vertical sidewalls (D990). The small black rectangles indicate the location of the tracer emission lines. The width of the road in all cases is 36 m. Adapted from Heist et al. (2009).

(D630), and a 9 m deep depressed roadway with vertical sidewalls (D990). Observations of flow and dispersion for these configurations were compared with those from the flat roadway case (FLAT). The width of the road in all cases is 36 m (full scale) and the width of the opening in D630 case is around 57 m (full scale). The letter 'D' in a case name stands for 'Depressed', the first single digit number represents the depth of the road in meters, and the two-digit number at the end of a case name denotes the angle between the sidewalls and the roadbed, in degrees.

Laser Doppler Velocimetry (LDV) was used for all velocity measurements in this study, details of which are described in Heist et al. (2009). The roughness length z_0, the friction velocity (u_*), and the displacement height (dh) were assessed by fitting the standard logarithmic velocity profile to the near surface measured upwind velocity profile in the FLAT case at $x = -16.75H$:

$$U(z) = \frac{u_*}{\kappa} \ln\left(\frac{z - dh}{z_0}\right) \quad (1)$$

where κ is the von Karman constant, taken to be 0.4. The values of u_*, z_0, and dh were calculated to be 0.17 m/s, 0.10 m and 0 m, respectively.

The tracer gas used in the study was high-purity ethane (C_2H_6) which is only slightly heavier than air. The flow rate of the tracer gas is 1500 cc/min. All samples were drawn through Rosemount Model 400A hydrocarbon analyzers. The concentrations of ethane were normalized to give the non-dimensional concentration $\chi = CU_r/(Q/L_xL_y)$, where C is the concentration (a fraction by volume) with background concentration subtracted, U_r is the reference wind speed (equal to 2.46 m/s, measured at a full-scale equivalent height of 30 m), Q is the volumetric effluent rate (1500 cm^3/min of ethane), L_x is the alongwind dimension of the roadway segment (24 cm, 36 m full scale), and L_y is the lateral length of the source segment (48 cm, 72 m full scale). In this study, we focus on concentrations associated with infinitely long line sources. As explained by Heist et al. (2009), the infinite line source results are constructed by superposition of concentrations resulted from five finite line segments placed laterally next to each other. Finally, the length scale, H, used throughout the study is 6 m (full scale).

2.2. Experimental results

2.2.1. Impact of road depression on the velocity field

The impact of road configurations on the flow field is shown in Fig. 3. We see that the depressions modify the flow field relative to that of the FLAT case. Roadways with vertical sidewalls (D690 and D990) create recirculating flow in the depressed regions, with a stronger recirculation in the deeper road cut case (D990). The D630 case, with angled sidewalls, has the least effect on the flow field, showing little evidence of recirculation in the depressed region.

The vertical profiles of horizontal velocity in the FLAT case, shown in Fig. 4, indicate that the horizontal wind speed increases with downwind distance from the road. This acceleration is caused by the absence of roughness blocks in the region *-16.75H* to *44.25H*, which includes the measurement zone. Due to conservation of ethane mass, the acceleration of the air flow causes a reduction in concentration over downwind distance that adds to that caused by vertical dispersion. Because the acceleration of the air flow occurs in all the cases, we assume that the concentration reduction in the depressed roadway cases compared to the flat case is caused primarily by the effects of the depression.

2.2.2. Impact of road depression on the turbulence field

Since the turbulence field plays a significant role in dispersion of traffic-related emissions (Tong et al., 2015), it is useful to examine the impact of different road configurations on Turbulent Kinetic Energy (TKE) values relative to those for the FLAT case. Fig. 5 shows the downwind variation of the square root of the ratio of TKE of depressed cases to that of flat terrain at $z = H/2$. This figure clearly indicates that the depression in the road is a source of shear generated turbulence, which causes the TKE to remain larger than that of flat terrain for the entire domain. As expected, the TKE of D990 is almost always larger than that of D690. The TKE in the D630 case exceeds that of D990 beyond $x = 20H$.

2.2.3. Impact of road depression on the concentration field

Concentrations considered in this study are concentrations observed downwind of the simulated freeways and at the same level with surroundings. For the FLAT, D690, and D990 cases, it corresponds to concentrations measured at $x \geq 3H$, and for the D630 case, it corresponds to those at $x \geq 4.75H$. Fig. 6 shows the variation of surface concentrations with downwind distance for the different cases. The left panel shows the differences between the surface concentrations of the FLAT case and the depressed cases as a function of downwind distance. The right panel focuses on the differences in surface concentrations among the depressed roadway cases close to the road. All the configurations decrease surface concentrations relative to those in the flat terrain case. The relative concentration reduction is highest for D990 case with the value of 80% very close to the road, $x = 3H$. As expected, the surface concentrations in D990 are lower than those in D690. The surface concentrations downwind of the road in D630 are higher than those of D990 everywhere except at $x = 15H$, where the surface concentration of D630 case is 95% of that of D990. As expected, the effects of road configurations on dispersion of roadway-emitted pollutants decreases with downwind distance from the edge of the depression. For example, the surface concentration reduction of D990 relative to flat terrain at $x = 3H$ is 80%, while that at $x = 40H$ is only 24%. But the distance over which the concentration approaches the flat terrain case varies with road configuration. For example, the surface concentration ratio of D990 to D690 at $x = 3H$ is 0.83, where the effect of configuration is large, while that at $x = 40H$ is 0.95.

3. Framework for the depressed road models

The wind tunnel results show that the depressed roadways 1) induce complex patterns, which includes recirculation within depressed roadways with vertical walls and 2) increase turbulence levels downwind of the depression relative to the FLAT case. In our modeling approach, we do not include these effects explicitly, but examine parameterizing them within the framework of a dispersion model applicable to flat terrain.

3.1. Modified van Ulden model

3.1.1. Model development

Our first analysis of the experimental results is based on a model

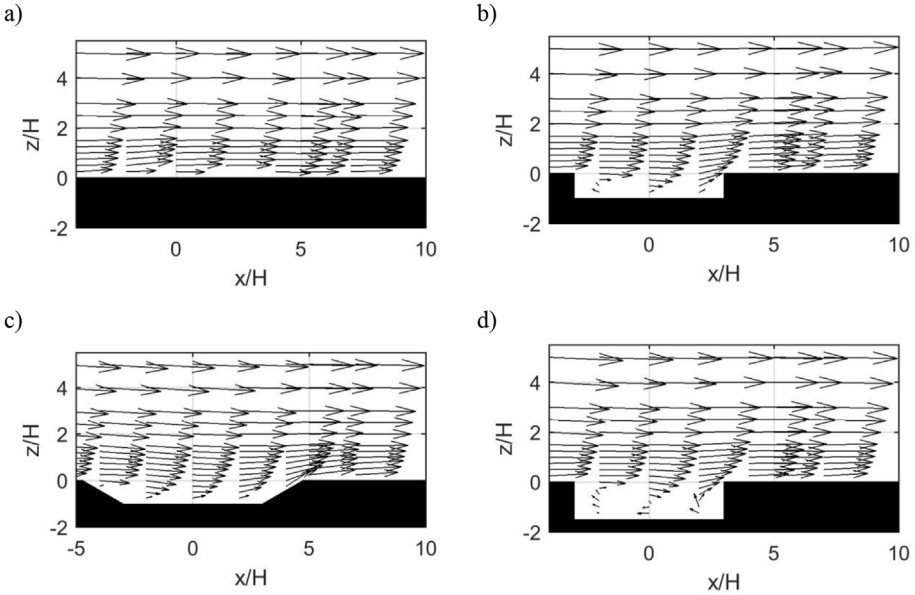

Fig. 3. Observed mean velocity vectors for a) FLAT, b) D690, c) D630, and d) D990 cases.

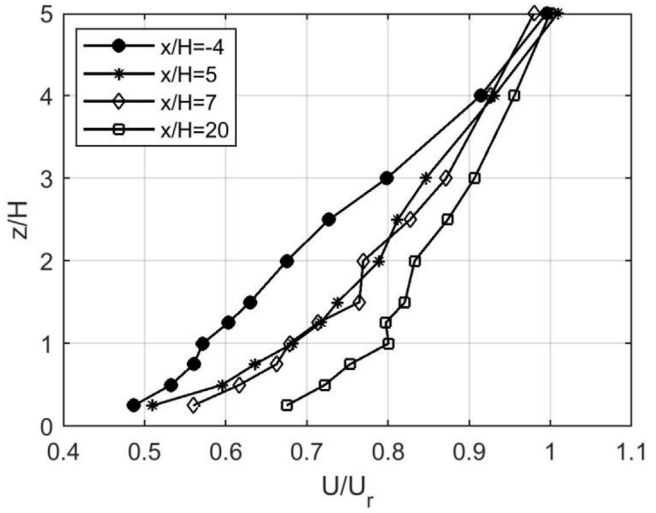

Fig. 4. Observed vertical profiles of horizontal velocity at multiple downwind locations in FLAT case. The air speed increases as air travels downwind.

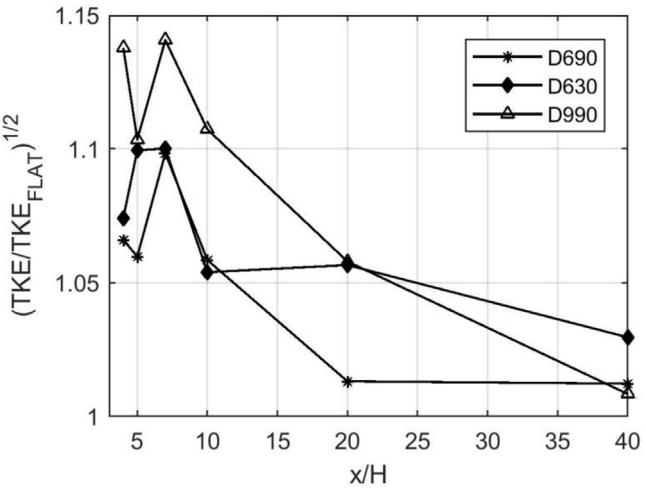

Fig. 5. Gradient of square root of observed TKE values of a) D690, b) D630, and c) D990 cases, normalized by the corresponding values observed at flat terrain case.

proposed by van Ulden (1978), which has been evaluated with observations from the Prairie Grass experiment (Barad, 1958). This model, which is the analytical solution of the eddy diffusivity-based mass conservation equation, expresses the concentration associated with a point source with strength Q (unit: $g.\ s^{-1}$). We use this model to estimate the concentration associated with an infinitely long line source with strength q (unit: $g.\ s^{-1}m^{-1}$), as

$$C(x,z) = \frac{Aq}{\overline{U}\overline{z}} \exp\left(-\left(\frac{Bz}{\overline{z}}\right)^{s}\right) \tag{2}$$

where the value of s depends on stability (Nieuwstadt and van Ulden, 1978b). A and B values are constant and depend only on s (van Ulden, 1978), $\overline{z}$ is the mass-weighted plume height defined as

$$\overline{z}(x) = \frac{\int_0^\infty zC(x,z)dz}{\int_0^\infty C(x,z)dz} \tag{3}$$

and $\overline{U}$ is the mass-weighted plume velocity defined by

$$\overline{U}(x) = \frac{\int_0^\infty U(z)C(x,z)dz}{\int_0^\infty C(x,z)dz} \tag{4}$$

We found that the shape of the observed vertical concentration profiles of all cases at various downwind distances are best reproduced by $s = 1.3$. This value of s agrees well with the values reported for neutral conditions by Nieuwstadt and van Ulden (1978a, b). The comparison of the observed vertical concentration profiles of the FLAT case with estimates of the formulation with $s = 1.3$ and $s = 2$ are shown in Figure S1 and Figure S2, respectively. Throughout this section, we assume that $s = 1.3$ which results in $A = 0.8$ and $B = 0.74$. The plume spread is related to the mean plume height by

$$\sigma_z = f_z\overline{z} \tag{5}$$

where f_z is also a function of the shape factor with the value of $f_z = 1.34$ for $s = 1.3$ (Venkatram, 2004). The growth of $\overline{z}$ with x is given by the equation derived by van Ulden (1978):

$$\frac{d\overline{z}}{dx} = \frac{K(q\overline{z})}{U(q\overline{z})q\overline{z}} \tag{6}$$

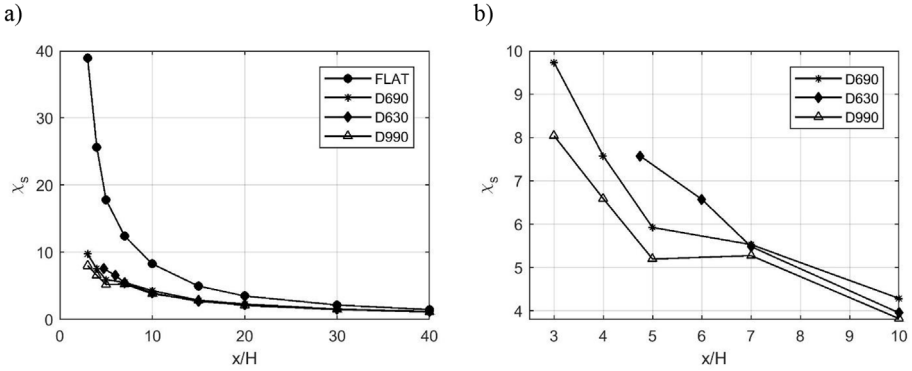

Fig. 6. Measured surface concentration as a function of downwind distance for different road configurations. Left plot includes flat terrain concentrations.

Table 1
Values of empirical parameters of different cases that form the σ_z expression in the van Ulden model with s = 1.3 and $p = 1/7$.

Case	$h_0(m)$	β
FLAT	1.2	1.00
D690	4.8	1.12
D630	3.6	1.37
D990	5.9	1.31

where $K(z)$ is the eddy diffusivity and $q = 1.54$ when $s = 1.3$.

Following van Ulden (1978), we assume that the wind speed, $U(z)$, can be written by a power law.

$$U(z) = U_r\left(\frac{z}{z_r}\right)^p \tag{7}$$

where $U_r = 2.46\ m/s$ is the reference velocity at the reference height $z_r = 30\ m$ (full scale) above the wind tunnel floor. We obtain the value of p by fitting equation (7) to the vertical profiles of wind speed in the wind tunnel. As discussed in section 2.2.1, the absence of roughness blocks results in change in the shape of the vertical profiles of horizontal velocity, which in turn results in p varying over distance. It turns out that the upwind velocity follows a power law with $p = 1/4$ and velocity profiles at different downwind distances follow power law functions with p ranging from 1/7 to 1/4; p decreases with increasing downwind distance. We use $p = 1/7$ for the rest of our analysis. It is shown that the final conclusions of our analysis remain the same if $p = 1/4$ (Table S1). However, we should note that the model assumes a constant p value while the wind tunnel velocity measurements show that p varies over distance.

By substituting equation 7 into 6 and assuming that the eddy diffusivity corresponds to the neutral expression $K(z) = \kappa u_* z$, where von Karman constant is $\kappa = 0.4$, we can integrate equation (6), assuming that the initial vertical plume spread is h_0,

$$\overline{z} = \left[\beta\frac{(p+1)}{q^p}\kappa\frac{u_*}{U_r}z_r^p x + \left(\frac{h_0}{f_z}\right)^{p+1}\right]^{\frac{1}{p+1}} \tag{8}$$

Although it is not used explicitly in our analysis, we present the associated equation for the more familiar measure of vertical spread, σ_z, as a function of x and h_0,

$$\sigma_z = \left[\beta\frac{(p+1)f_z^{p+1}}{q^p}\kappa\frac{u_*}{U_r}z_r^p x + h_0^{p+1}\right]^{\frac{1}{p+1}} \tag{9}$$

Note that $p = 1/7$ results in $\sigma_z \sim x^{7/8}$ when h_0 is small.

We account for the effects of the depressed road through two parameters: a factor β which multiplies the flat terrain friction velocity in equation (9) and an initial vertical plume spread h_0. The values of these parameters are obtained by fitting results from the modified van Ulden model to the near-surface concentration measurements made in the wind tunnel. It is important to note that only two parameters are used to fit entire range of surface and elevated concentrations associated with each of the road configurations.

3.1.2. Estimation of the empirical parameters

Concentrations downwind of the freeway were modeled as the sum of concentrations due to six individual line sources, the same number of line sources in the wind tunnel (Heist et al., 2009). For each case, we fit the near-surface concentrations estimated by the modified van Ulden model to those observed in the wind tunnel to obtain the values of the two parameters, β and h_0. The values of these parameters are listed in Table 1. These values suggest that it is necessary to use an initial vertical dispersion of 1.2 m to describe the concentrations for the flat terrain case. A 6 m depressed roadway with straight edges adds 3.7 m to the initial vertical dispersion of flat terrain, while a 9 m depressed roadway with straight edges adds 4.8 m. The D630 case adds 2.4 m to the flat terrain initial vertical dispersion, indicating the smaller role of turbulent mixing in the presence of sloping walls. This suggests that one effect of the road depression is to increase the initial vertical dispersion. This is consistent with the method used in CALINE2 to account for roadway depression (Benson, 1992).

The second effect of the road depression is an increase of β, which is interpreted as an increase in the rate of vertical plume spread or turbulence levels. The D690, D630, and D990 cases result in increases of 12%, 37%, and 31% in this rate compared to those of flat terrain, respectively. This is consistent with the results shown in Fig. 5, where larger values of TKE were observed in depressed cases compared to the FLAT case. The highest rate for the D630 case is attributed to the vertical velocities induced by the upward slope of the downwind edge of the depression. Fig. 3 appears to support this hypothesis. It should be noted that the model does not take into account the impacts of vertical components of the wind velocity on downwind concentrations. Therefore, these effects are indirectly included in the empirical parameters of the model.

3.2. Modified RLINE based model

3.2.1. Model development

As discussed earlier, one of the objectives of this research is to enable the RLINE model to estimate concentrations downwind of the depressed roadways. In this section we suggest modifications to the RLINE model to account for the effects of depressed roads on dispersion. RLINE (Snyder et al., 2013) is designed for estimating surface concentrations close to roadways. It is based on a steady-state Gaussian formulation and treats a line source as a set of point sources and integrates over the differential concentrations at the receptor due to each point source (Snyder et al., 2013). This model differs from the van

Table 2
Values of empirical parameters of different cases that form the σ_z expression in RLINE model.

Case	$h_0(m)$	α
FLAT	0.4	1.00
D690	4.0	1.67
D630	3.5	1.87
D990	4.8	1.83

Ulden model in two ways: 1) it assumes that the vertical distribution of concentration is a normal (Gaussian) distribution, and 2) the velocity profile follows a logarithmic profile (equation (1)).

We estimate near-surface concentrations by modifying RLINE using the two parameters described in the previous section. The vertical spread of the plume in RLINE under neutral conditions is modified as follows,

$$\sigma_z = \sqrt{\sigma_{z_F}^2 + h_0^2};\ \sigma_{z_F} = 0.57\alpha\frac{u_*}{U(\bar{z})}x \tag{10}$$

where σ_{z_F} is computed using the formulations derived by (Venkatram et al., 2013) for neutral conditions. As before, we account for the effects of the depressed road through two parameters: a factor α for increasing turbulence, and initial vertical dispersion, h_0, in the presence of the road depression. We adjust α and the initial vertical dispersion value for each case to find the best fit to the near-surface measured concentrations.

3.2.2. Estimation of the empirical parameters

Following the procedure in section 3.1.2, the magnitudes of h_0 and α for each case are calculated so that the near-surface concentrations estimated by the modified RLINE model are close to the observed values (Table 2). The enhancements in initial vertical dispersion and friction velocity of depressed cases in the modified RLINE follow the same trend as those in the modified van Ulden model, although the magnitudes are different in the two models. The differences in magnitudes are related to the differences in the horizontal velocity and concentration profiles used in the two models. While the initial vertical dispersion is calculated to be 0.4 m for the FLAT case, the value of this parameters increases to 4.0 m, 3.5 m, and 4.8 m for the D690, D630, and D990 cases. As in the application of the modified van Ulden model, the largest increase in turbulence levels is in the D630 case ($\alpha = 1.87$), while the smallest increase occurs in the D690 case ($\alpha = 1.67$).

4. Comparison of the modified models with observations

After obtaining the empirical values of the two parameters using surface concentrations, we evaluated the performance of the model in describing concentrations above the surface. Model performance was characterized using the following statistical parameters: the logarithmic mean of the ratios of the observed concentration to the estimated concentration, m_g, the logarithmic standard deviation of the ratios, s_g, the fraction of estimated concentrations that lie between 0.5 and 2 times the observed concentrations (fac2), the correlation coefficient (r^2) (Venkatram and Horst, 2006), and normalized mean square error (NMSE) (Chang and Hanna, 2004).

4.1. Modified van Ulden model

The performance of the model to explain observed concentrations at all elevations is shown in Fig. 7. This figure indicates that the modified van Ulden model provides a good description of the concentrations at all heights measured downwind of the roadway. The model underestimates the low values of concentrations in the FLAT case and overestimates the low values in the D690 and the D990 cases.

Fig. 8 shows the comparison of model estimates of the concentration profiles for the D690 case with corresponding measurements at several downwind distances. The good description of the observations provided by the model reinforces the result that only two parameters are needed to describe the entire concentration field downwind of the depressed roads.

Fig. 9 compares the variation in the observed vertical concentration profiles of the FLAT and D690 cases at $x = 3H$ with the corresponding modeled values. The two parameters allow us to capture the differences in vertical concentration profiles of the different cases. The NMSE corresponding to the FLAT case is 0.05 and that for the D690 case is 0.02.

4.2. Modified RLINE based model

It turns out (Figure S2 in supplementary material) that estimates from the Gaussian distribution ($s = 2$) in RLINE deviate from observed concentrations above the surface. Because the height that is relevant to exposure to pollutant concentrations is about 3 m, we compare the modified RLINE model predictions with the corresponding concentrations observed below $z = 6\,m$ using the parameter values listed in Table 2. Fig. 10 shows that the scatter at $x/H = 4$ (top left panel) is not small, but the 95% confidence interval ($\sim s_g^2$) of the ratio of the modeled to observed concentrations is less than a factor of 1.2 at other downwind distances.

Fig. 11 compares the vertical profiles estimated from the modified RLINE with the measured vertical concentration profiles at multiple downwind distances for the D690 case. Comparing this figure with Fig. 8 reinforces the fact that while estimates from modified RLINE model are acceptable near ground-level, they do not follow the vertical profiles of the measured concentrations.

5. Discussion

It is informative to compare the relative magnitudes of the mitigation effects induced by the depressed road with those related to solid barriers (Heist et al., 2009). We consider a road with one 6 m tall barrier downwind of the road and another with a 6 m tall solid barrier on each side of the road. Fig. 12 shows the ratio of surface concentrations downwind of roads with one (two) noise barrier(s) to those downwind of the road in the D690 case, where the width of all roads are $6H$ and the origin is located at the center of the simulated roads. The ratio of surface concentrations downwind of two noise barriers to those of the depressed road ranges from 0.80 to 1.08, while the ratio for the single downwind solid barrier ranges from 0.96 to 1.15 (Fig. 12). The 6 m double noise barrier is more effective than the depressed road close to the road (up to $x = 10H$) because of the strong recirculation zone behind the downwind solid barrier. The depressed road is more effective further downwind. The 6 m deep depressed road is more effective than a single 6 m downwind solid barrier for most downwind distances.

6. Summary and conclusions

We analyze data from a wind-tunnel study (Heist et al., 2009) to suggest modifications to flat terrain dispersion models to account for the effects of depressed roadways on dispersion. We show that increasing the friction velocity and initial vertical dispersion in a flat terrain model proposed by van Ulden (1978) captures most of the effects induced by depressed roadways. We find that the van Ulden model with $s = 1.3$ provides the best fit to the vertical concentration profiles observed downwind of all roadways under neutral conditions. Similar modifications to the RLINE (Snyder et al., 2013) model also provide good descriptions of near-surface concentrations measured downwind of the depressed roadway configurations in the wind tunnel (Heist et al., 2009).

The friction velocity and initial vertical dispersion used to account for the effects of the depressed roadway increase with the depth of the

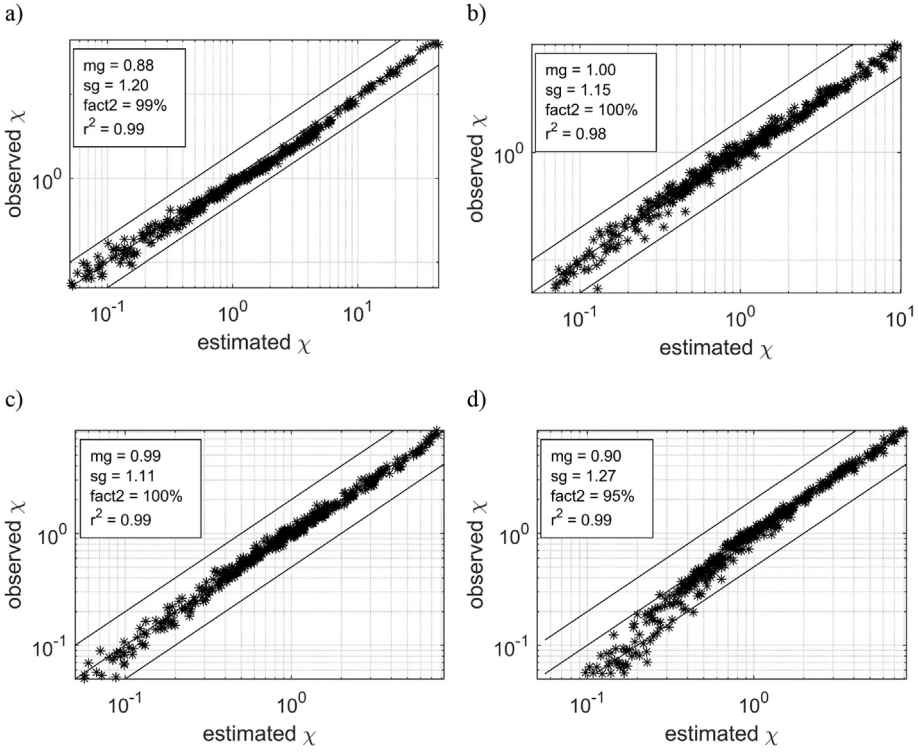

Fig. 7. Comparison of the modified van Ulden model estimates (with s = 1.3 and p = 1/7) with observed concentrations for all downwind distances and all heights; a) FLAT case, b) D690 case, c) D630 case, and d) D990 case.

depressed roadway. At this point, we do not have enough data to suggest a general formula to estimate these increases. However, the empirical results from our study are relevant to modeling the effects of depressed roadways that lie in the range of 6–9 m. The concentrations associated with emissions from these roadways can be estimated by increasing the friction velocity corresponding to flat terrain by a factor of 1.8 and using an initial vertical dispersion of about 4 m. This work provides a foundation for future studies that can result in development

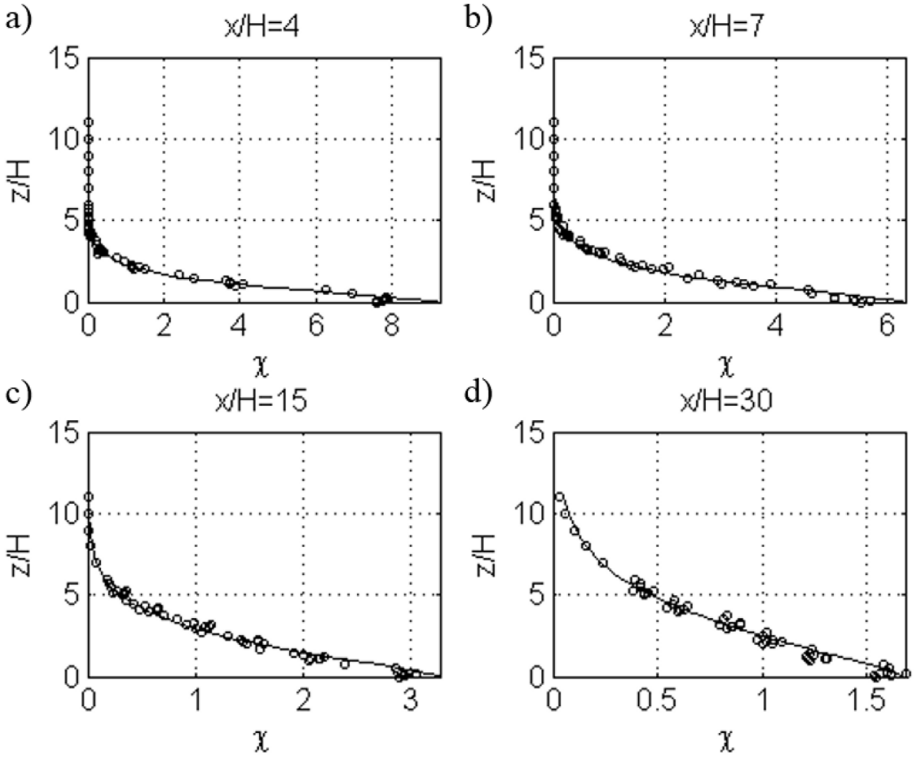

Fig. 8. Comparison of the vertical concentration profiles at multiple downwind locations predicted by the modified van Ulden model (with s = 1.3 and p = 1/4) with those of the observations (D690 case).

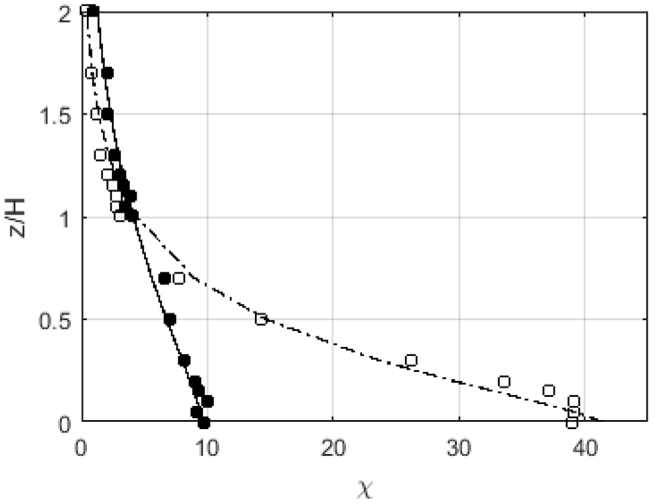

Fig. 9. Performance of the modified van Ulden model (with s = 1.3 and p = 1/7) in predicting vertical concentration profiles of the FLAT and D690 cases at x = 3H. (Open squares – measured flat terrain, solid circles – measured D690, dashed line – modeled flat terrain, and solid line – modeled D690).

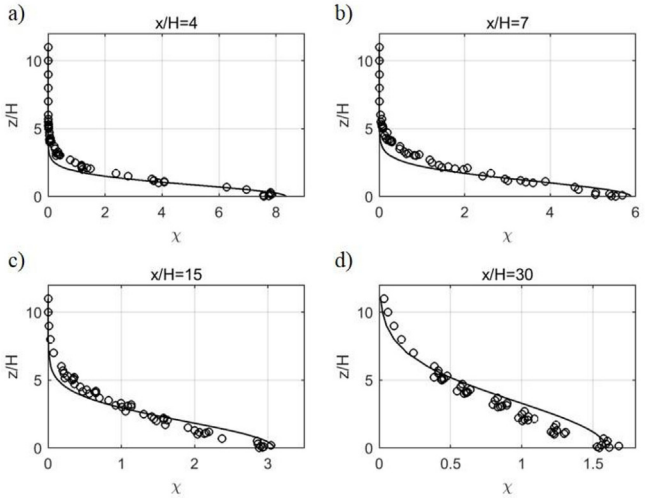

Fig. 11. Comparison of the vertical concentration profiles at multiple downwind locations predicted by the modified RLINE model with those of the observations (D690 case). Open circles are the observed values.

of a depressed roadway dispersion model formulation.

The width of the opening at the top of the depression and the width of the roads are not taken into account in the model formulation because the widths of the roads in all cases were the same. But we expect that the mitigation effects of depressed roadways decrease as the ratio of the width to the depth of the depression (W/D) becomes large, and street canyon effects become important when this ratio becomes small (Berkowicz, 2000; Schulte et al., 2015).

It should be noted that the results reported in this paper might be functions of atmospheric stability, a topic that is not examined in this paper. Also, along highway concentrations are not addressed in this study. However, previous studies have reported that channeling and eddying effects decrease the rate of pollutant transport out of the depressed zone, causing an increase of along-highway concentrations (Benson, 1992).

This paper shows that the effects of the complex flow patterns induced by the depressed road on dispersion can be simulated through simple modifications to a flat terrain model such as RLINE. This conclusion is supported by the empirical results from the Caltrans study that led to the modification in CALINE2 (Benson, 1992). In another study next to a depressed highway in Las Vegas (Baldauf et al., 2013),

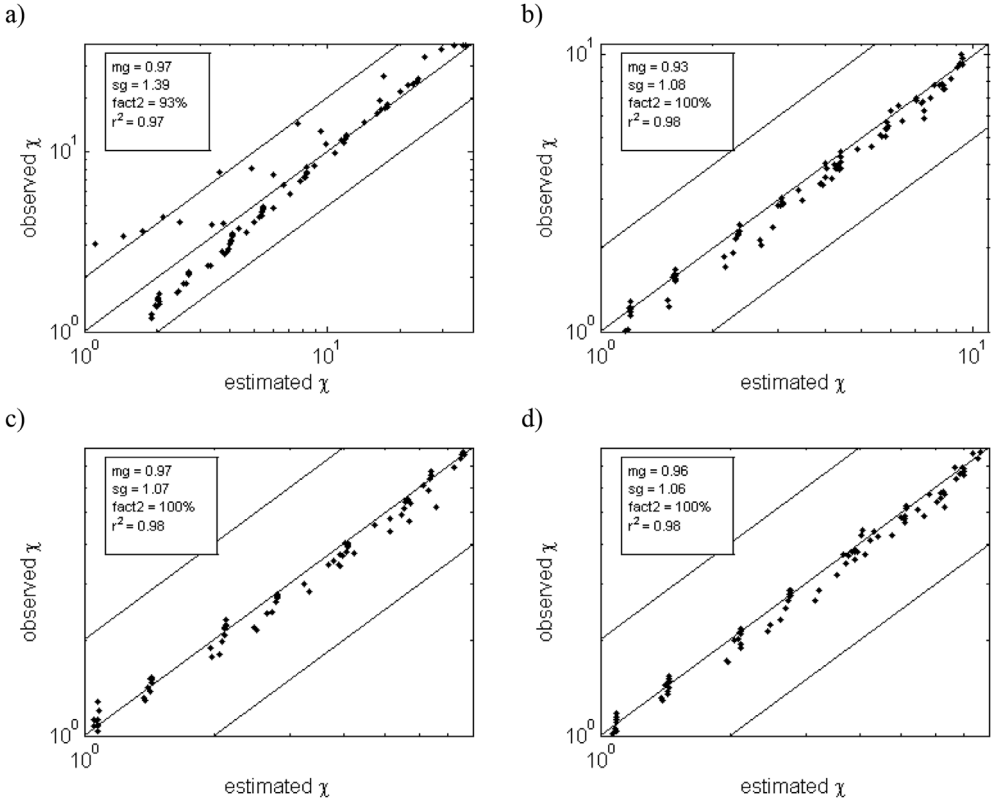

Fig. 10. Comparison of the modified RLINE model estimates with observed concentrations below 6 m height for x/H = 4, 7 (top panels) and x/H = 15, 30 (bottom panels).

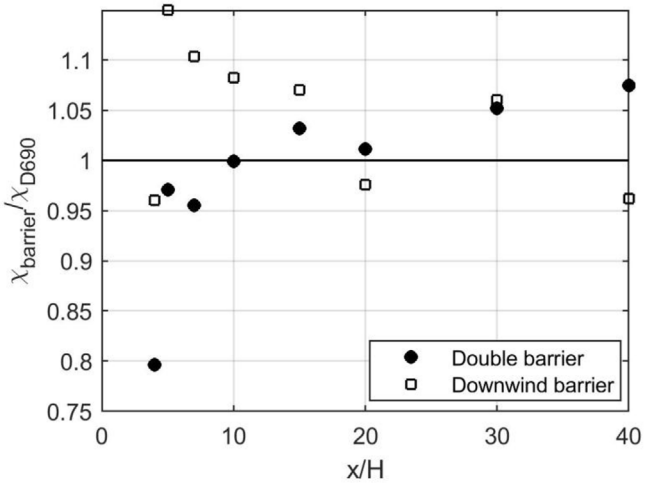

Fig. 12. Ratio of surface concentrations measured downwind of barrier cases to those of D690 case over downwind distance. (Solid circle corresponds to 6 m double solid barriers and open square corresponds to 6 m downwind barrier).

the observed concentrations were described well by assuming that the initial vertical dispersion of the plume is roughly equal to the depression of the road, which was approximately 5 m at the location of the measurements.

The major contribution from this study is that the entire concentration field-surface concentrations and vertical profiles-downwind of a depressed highway can be described through two simple modifications of a dispersion model designed for flat terrain. The two parameters corresponding to these modifications are related to the geometry of the depression. For example, the height of the initial plume spread can be modeled using the approach in Schulte et al. (2015) so that $h_0 = aD/(b + a_r)$ where a and b are empirical constants, and the aspect ratio, $a_r = D/W$. This formulation ensures that the initial plume spread is controlled by the depth, D, when W is large, and by W when D is relatively large as in a deep street canyon.

Disclaimer

The views expressed in this article are those of the authors and do not necessarily represent the views or policies of the U.S. Environmental Protection Agency. Any mention of trade names, products, or services does not imply an endorsement by the U.S. Government or the U.S. Environmental Protection Agency.

Appendix A. Supplementary data

Supplementary data related to this article can be found at http://dx.doi.org/10.1016/j.atmosenv.2018.04.058.

References

Ahangar, F.E., Heist, D., Perry, S., Venkatram, A., 2017. Reduction of air pollution levels downwind of a road with an upwind noise barrier. Atmos. Environ. 155, 1–10. http://dx.doi.org/10.1016/j.atmosenv.2017.02.001.

Amini, S., Ahangar, F.E., Schulte, N., Venkatram, A., 2016. Using models to interpret the impact of roadside barriers on near-road air quality. Atmos. Environ. 138, 55–64. http://dx.doi.org/10.1016/j.atmosenv.2016.05.001.

Amini, S., Venkatram, A., Heist, D.K., Perry, S.G., 2017. Modeling the dispersion of pollutants in vicinity of depressed roadways. In: Proceedings of the Air and Waste Management Association's Annual Conference and Exhibition, AWMA.

Baldauf, R.W., Heist, D., Isakov, V., Perry, S., Hagler, G.S.W., Kimbrough, S., Shores, R., Black, K., Brixey, L., 2013. Air quality variability near a highway in a complex urban environment. Atmos. Environ. 64, 169–178. http://dx.doi.org/10.1016/j.atmosenv.2012.09.054.

Barad, M.L., 1958. Project Prairie Grass, a Field Program in Diffusion. Volume 1 (No. Grp-59-vol-1). Air Force Cambridge Res. Labs Hanscom AFB MA. http://dx.doi.org/10.1016/0022-460X(71)90105-2.

Bemis, G.R., Ranzieri, A.J., Benson, P.E., Peter, R.R., Pinkerman, K.O., Squires, B.T., 1977. Air Pollution and Roadway Location, Design, and Operation- Project Overview. FHWA-catl-7080-77-25. California Department of Transportation, Sacramento, CA.

Benson, P.E., 1992. A Review of the Development and Application of the Caline3 and 4 Models 26. pp. 379–390.

Berkowicz, R., 2000. OSPM - a parameterised street pollution model. Environ. Monit. Assess. 65, 323–331. http://dx.doi.org/10.1023/A:1006448321977.

Chang, J.C., Hanna, S.R., 2004. Air quality model performance evaluation. Meteorol. Atmos. Phys. 87, 167–196.

Feeney, P.J., Cahill, T.A., Flocchini, R.G., Eldred, R.A., Shadoan, D.J., Dunn, T., 1975. Effect of Roadbed Configuration on Traffic Derived Aerosols. J. Air Pollut. Contr. Assoc. 25 (11), 1145–1147. http://doi.org/10.1080/00022470.1975.10470190.

Ghasemian, M., Amini, S., Princevac, M., 2017. The influence of roadside solid and vegetation barriers on near-road air quality. Atmos. Environ. 170. http://dx.doi.org/10.1016/j.atmosenv.2017.09.028.

Hagler, G.S.W., Tang, W., Freeman, M.J., Heist, D.K., Perry, S.G., Vette, A.F., 2011. Model evaluation of roadside barrier impact on near-road air pollution. Atmos. Environ. 45, 2522–2530. http://dx.doi.org/10.1016/j.atmosenv.2011.02.030.

Health Effects Institute, 2010. Panel on the Health Effects of Traffic-Related Air Pollution. Traffic-related Air Pollution: a Critical Review of the Literature on Emissions, Exposure, and Health Effects. Health Effects Institute No. 17.

Heist, D., Isakov, V., Perry, S., Snyder, M., Venkatram, A., Hood, C., Stocker, J., Carruthers, D., Arunachalam, S., Owen, R.C., 2013. Estimating near-road pollutant dispersion: a model inter-comparison [WWW Document]. Transp. Res. Part D Transp. Environ. http://dx.doi.org/10.1016/j.trd.2013.09.003.

Heist, D.K., Perry, S.G., Brixey, L. a, 2009. A wind tunnel study of the effect of roadway configurations on the dispersion of traffic-related pollution. Atmos. Environ. 43, 5101–5111. http://dx.doi.org/10.1016/j.atmosenv.2009.06.034.

Irwin, H.P.A.H., 1981. The design of spires for wind simulation. J. Wind Eng. Ind. Aerod. 7 (3), 361–366. http://doi.org/10.1016/0167-6105(81)90058-1.

Nieuwstadt, F.T.M., van Ulden, A.P., 1978a. A numerical study on the vertical dispersion of passive contaminants from a continuous source in the atmospheric surface layer. Atmos. Environ. 12, 2119–2124. http://dx.doi.org/10.1016/0004-6981(78)90166-X.

Nieuwstadt, F.T.M., van Ulden, A.P., 1978b. A numerical study of the vertical dispersion of passive contaminants from a continuous source in the atmospheric surface layer. Atmos. Environ. 14, 267–269. http://dx.doi.org/10.1016/0004-6981(80)90288-7.

Schulte, N., Snyder, M., Isakov, V., Heist, D., Venkatram, A., 2014. Effects of solid barriers on dispersion of roadway emissions. Atmos. Environ. 97, 286–295. http://dx.doi.org/10.1016/j.atmosenv.2014.08.026.

Schulte, N., Tan, S., Venkatram, A., 2015. The ratio of effective building height to street width governs dispersion of local vehicle emissions. Atmos. Environ. 112, 54–63. http://dx.doi.org/10.1016/j.atmosenv.2015.03.061.

Snyder, W.H., 1979. The EPA Meteorological Wind Tunnel: Its Design, Construction, and Operating Characteristics. U.S. Environmental Protection Agency, Research Triangle Park, NC Report No. EPA-600/4-79-051.

Snyder, M.G., Venkatram, A., Heist, D.K., Perry, S.G., Petersen, W.B., Isakov, V., 2013. RLINE: a line source dispersion model for near-surface releases. Atmos. Environ. 77, 748–756. http://dx.doi.org/10.1016/j.atmosenv.2013.05.074.

Steffens, J.T., Heist, D.K., Perry, S.G., Isakov, V., Baldauf, R.W., Zhang, K.M., 2014. Effects of roadway configurations on near-road air quality and the implications on roadway designs. Atmos. Environ. 94, 74–85. http://dx.doi.org/10.1016/j.atmosenv.2014.05.015.

Tong, Z., Whitlow, T.H., MacRae, P.F., Landers, A.J., Harada, Y., 2015. Quantifying the effect of vegetation on near-road air quality using brief campaigns. Environ. Pollut. 201, 141–149. http://dx.doi.org/10.1016/j.envpol.2015.02.026.

U.S. Environmental Protection Agency, 2016. Technical Support Document (TSD) for Replacement of CALINE3 with AERMOD for Transportation Related Air Quality Analyses. Report No. EPA- 454/B-16–1006, December.

van Ulden, A.P., 1978. Simple estimates for vertical diffusion from sources near the ground. Atmos. Environ. 12, 2125–2129. http://dx.doi.org/10.1016/0004-6981(78)90167-1.

Venkatram, A., 2004. On estimating emissions through horizontal fluxes. Atmos. Environ. 38, 1337–1344. http://dx.doi.org/10.1016/j.atmosenv.2003.11.018.

Venkatram, A., Horst, T.W., 2006. Approximating dispersion from a finite line source. Atmos. Environ. 40, 2401–2408. http://dx.doi.org/10.1016/j.atmosenv.2005.12.014.

Venkatram, A., Snyder, M., Isakov, V., Kimbrough, S., 2013. Impact of wind direction on near-road pollutant concentrations. Atmos. Environ. 80, 248–258. http://dx.doi.org/10.1016/j.atmosenv.2013.07.073.